Increased Karyopherin Alpha Levels Attenuate Mutant Ataxin-1-Induced Neurodegeneration

Elena K Ruff[1,2,4], Dylan Lawrence Timperman[1,2,4], Adulfo Anaya Amador[1,2], Isabella Aguirre-Lamus[1,2], Maria de Haro[1,2], Ismael Al-Ramahi[1,2,3,5]

[1] Jan and Dan Duncan Neurological Research Institute, Texas Children's Hospital, Houston, United States.
[2] Department of Molecular and Human Genetics, Baylor College of Medicine, Houston, United States.
[3] Center for Alzheimer's and Neurodegenerative Diseases, Baylor College of Medicine, Houston, United States.
[4] These authors contributed equally to the publication
[5] Corresponding author: ismael.alramahi@bcm.edu

Abstract
Neurodegenerative diseases are characterized by the abnormal accumulation of disease-driving proteins. Emerging evidence suggests that nucleocytoplasmic transport (NCT) components play a critical role in neurodegeneration. This study investigates the impact of modulating Karyopherin alpha (KPNA) levels on neurodegeneration induced by mutant Ataxin-1 (ATXN1) using a *Drosophila* model of Spinocerebellar Ataxia Type 1 (SCA1). Our findings reveal that ATXN1 (82Q) interacts with KPNAs in the nucleus and cytoplasm of neurons. Increasing KPNA levels alleviates ATXN1 (82Q)-induced neurodegeneration and progressive neuronal dysfunction. Surprisingly, mechanistic analyses demonstrate that elevated KPNA levels retain mutant ATXN1 in the cytoplasm, reducing its nuclear accumulation in the *Drosophila* central nervous system. Moreover, elevated KPNA levels lead to a decrease in soluble oligomeric ATXN1. These results indicate that KPNAs may act as chaperones for mutant ATXN1, preventing its nuclear translocation and reducing its pathological effects. Importantly, they also constitute a proof of principle that retaining mutant ATXN1 in the cytoplasm represents an attractive and viable therapeutic option. Given the dysregulation of Karyopherins in many neurodegenerative diseases and their emerging role as chaperones, the results presented here may extend beyond SCA1 into other disorders like Alzheimer's or Parkinson's disease.

Introduction
A common hallmark of neurodegenerative diseases, though characterized by a number of different cognitive, psychological, or motor clinical manifestations, is the abnormal accumulation of disease-driving proteins (Kovacs, 2016; Tsoi et al., 2023). The majority of neurodegenerative diseases progress in an irreversible manner and currently have no effective treatments (Hou et al., 2019).
Growing evidence shows that nucleocytoplasmic transport (NCT) plays a key role in neurodegenerative diseases (Ding & Sepehrimanesh, 2021). In ALS and FTLD, for example, impaired NCT is identified as a major mechanism of disease. TDP-43, the disease protein identified in 97% of ALS and FTLD cases, mislocalizes and aggregates in the cytoplasm of neurons (Neumann et al., 2006; Arai et al., 2006; Winton et al., 2008; Hergesheimer et al., 2019; Ionescu et al., 2023). These TDP-43 aggregates also contain Nucleoporins (Nups) and NCT factors, contributing to further dysregulation of NCT (Girdhar & Guo, 2022). Evidence suggests that NCT dysregulation is a major mechanism in AD as well (Eftekharzadeh et al. 2018; Ding & Sepehrimanesh, 2021). Invaginations and abnormalities of the nuclear envelope, in conjunction with abnormal localization of importins, Nups and RanGDP in AD patient brains

add to this growing evidence (Girdhar & Guo, 2022; Eftekharzadeh et al., 2018; Lee et al., 2006; Moore et al., 2020; Eftekharzadeh et al., 2018; Ding & Sepehrimanesh, 2021; Coyne & Rothstein, 2022; Sohn et al., 2023; Frost et al., 2016). Karyopherins (KPNs), i.e., importins, exportins, and transportins, are the family of proteins that facilitate nuclear transport. Alpha KPNs (KPNAs) bind NLS sequences and are then carried by Beta KPNs (KPNBs) into the nucleus, together with their cargo. This process also necessitates Nups, Ran, and RanGTPases (Gorlich et al., 1996; Aramburu & Lemke, 2017; Fallini et al., 2020). There are several human KPNs, each of which associates with a specific set of cargos (Ding & Sepehrimanesh, 2021). Many of these KPNs are dysregulated in ALS, FTD, AD, and HD (Pasha et al., 2021; Solomon et al., 2018; Lee et al., 2006; Woerner et al., 2016; Chan et al., 2011; Gasset-Rosa et al., 2017). Interestingly, importins, also called nuclear import receptors (NIRs), can reduce aggregation of TDP-43 and other RNA binding proteins in cell and animal models by acting as a chaperone for the toxic, aggregated protein (Guo et al., 2018; Khalil et al., 2022). It has been shown that NIRs can disaggregate TDP-43, increase its nuclear localization and mitigate its toxicity (Guo et al., 2018; March et al., 2016; Khalil et al., 2022).

Spinocerebellar Ataxia Type 1 (SCA1) is one of 9 Polyglutamine diseases (polyQ) caused by the expansion of a translate CAG tract in the *ATXN1* gene (Huang et al., 2019; Zoghbi & Orr, 1995). This polyQ expansion causes a toxic gain of function in the protein, which misfolds and accumulates in the nuclei of neurons (Zoghbi & Orr, 2000). Notably, polyQ expansions can be understood as a type of low complexity domain (LCD) or Prion Like Domain (PrLD) (Zhang, Hinde, et al., 2020). ATXN1 itself has also been identified as a PrLD (March et al., 2016). ATXN1 aggregates are pathogenic when they localize to the nucleus and form nuclear bodies (NBs) (Klement et al., 1998; Zhang, Hinde, et al., 2020). PolyQ-expanded ATXN1 without its functional nuclear localization signal does not cause disease phenotypes in SCA1 mouse models (Klement et al., 1998; Handler et al., 2023). This indicates that nuclear localization of mutant ATXN1 is required for pathogenesis. Interestingly, the ATXN1 protein interactome includes many nuclear transport components (Zhang, Williamson, et al., 2020). Additionally, the presence of polyQ-ATXN1 disrupts the normal nucleocytoplasmic transport mechanisms. This includes inhibition of importins and exportins from binding their normal cargo, reducing the availability of RanGDP, and disrupting the nuclear pore complex (Zhang, Williamson, et al., 2020).

Here we explore the effect of modulating the levels of Karyopherin alpha (KPNA) on mutant ATXN1-induced neurodegeneration using a *Drosophila* SCA1 model. We show that ATXN1 (82Q) interacts with both *Drosophila* and human KPNAs both in the nucleus and in the cytoplasm of neurons. Surprisingly, we find that increased levels of KPNAs mitigate ATXN1 (82Q)-induced neurodegeneration and progressive neuronal dysfunction. Further mechanistic analysis reveals that increased KPNA levels cause the retention of ATXN1 in the cytoplasm and lowers ATXN1 levels in the nuclei of cells in the *Drosophila* central nervous system (CNS). Additionally, we find that increased KPNA levels also result in a decrease in soluble oligomeric ATXN1 levels. Taken together, our results support the notion that KPNAs can act as ATXN1 chaperones and may play similar roles in the context of other neurodegeneration driving proteins.

Results

KPNAs colocalize with ATXN1 (82Q) aggregates in the nucleus and the cytoplasm of neurons.

The ATXN1 interactome includes several NCT proteins, including KPNB3 and KPNA2 (Zhang, Williamson, et al., 2020) but the functional consequence of these interactions has not been fully characterized. In order to investigate the potential interaction between ATXN1 (82Q) and KPNAs *in vivo*, we expressed ATXN1 (82Q) alongside HA-tagged nuclear import receptors using the *nrv2-GAL4* CNS driver in *Drosophila* ventral nerve cords. Immunofluorescence was performed in order to visualize the protein localization. In control CNS, the ATXN1 (82Q) signal is found predominantly in the nucleus (**Figure 1B**). Co-expression of ATXN1 (82Q) alongside the HA-tagged *Drosophila* homolog of KPNA6 results in protein colocalization **(Figure 1C**). Interestingly, the signals from ATXN1 (82Q) and the *Drosophila* KPNA overlap in distinct aggregate shapes in both the nucleus and the cytoplasm (**Figure 1C**). A similar co-localization in the nucleus and cytoplasm is also observed when ATXN1 (82Q) is co-expressed with human KPNA2 or KPNA5 in the *Drosophila* CNS (**Figure 1D-E**). These results indicate that ATXN1 (82Q) interacts with *Drosophila* and human KPNAs *in vivo* and that this interaction happens both in the nucleus as well as in the cytoplasm of neurons.

Increased KPNA levels ameliorate ATXN1 (82Q)-induced neurodegeneration in Drosophila.

Since we see a colocalization of KPNAs with ATXN1 (82Q) aggregates, we next investigated the functional significance of this interaction. For this, we first used the *gmr-GAL4* driver for retinal ATXN1 (82Q) expression which leads to internal and external degenerative phenotypes (**Figure 2**). Interestingly, co-expression of ATXN1 (82Q) together with the *Drosophila* homologs of either KPNA4, KPNA2, or KPNA6 ameliorates the ATXN1 (82Q)-induced neurodegeneration (**Figure 2C-F and K-N**). The attenuation of the ATXN1 (82Q) phenotypes was robust both when analyzing external eye morphology as well as when investigating the internal photoreceptor structure. Co-expression of ATXN1 (82Q) together with human KPNA2 and KPNA5 also ameliorated ATXN1 (82Q)-induced neurodegeneration (**Figure 2G-H, O-P**).

To corroborate the phenotypic interaction between ATXN1 (82Q) and KPNAs in a time progressive assay, we analyzed the effect of co-expressing KPNAs together with ATXN1 (82Q) in the CNS using a behavioral test. Expression of ATXN1 (82Q) in the *Drosophila* CNS leads to progressive dysfunction which can be quantified using the motor performance (speed) of the animals as a function of age using a climbing assay (**Figure 3 Gray lines A-D**). We have used this assay to analyze toxic protein effects on neurons in other *Drosophila* models of neurodegenerative diseases **(**Park, J et al., 2013; Al-Ramahi et al., 2018**)**. Expression of ATXN1 (82Q) in the *Drosophila* CNS results in a progressive decline in motor function over time, compared to negative controls (**Figure 3 Blue lines**). Increasing the levels of either *Drosophila* or human KPNAs in the central nervous system significantly ameliorates this progressive ATXN1 (82Q)-induced neuronal dysfunction (**Figure 3 Red lines**).

Increased KPNA levels reduce overall nuclear ATXN1 (82Q) accumulation

Prior studies show that the interaction between KPNB and proteins with PrLDs that are mislocalized to the cytoplasm (like TDP-43, FUS, EWSR1, TAF15, hnRNPA1, and hnRNPA2) results in defibrilization and relocalization of these proteins to the nucleus (Guo et al., 2018, Pasha et al., 2021; Girdhar & Guo, 2022; Khalil et al., 2022; Fare et al., 2023). Furthermore, KPNB not only returns TDP-43 to the nucleus but can also suppress TDP-43-induced neurodegeneration (Khalil et al., 2022). However, in the case of ATXN1 (82Q), nuclear localization of the protein is linked to its toxic effects, since mutating the NLS in polyQ-expanded ATXN1 actually removes its pathogenicity in mice (Klement et al., 1998; Handler et al., 2023), therefore KPNA must be acting in a different way to suppress ATXN1 (82Q)-induced neurodegeneration. Other potential mechanisms of neuroprotection have been proposed for KPNs, including evidence supporting chaperoning and disaggregation functions (Guo et al., 2018; Pasha et al., 2021; Jäkel et al., 2002). Our immunofluorescence assays revealed that ATXN1 (82Q) physically interacts with KPNAs in the *Drosophila* CNS. Therefore, we performed ATXN1 immunofluorescence assays in animals expressing ATXN1 (82Q) either alone or in combination with the KPNAs that ameliorated neurodegeneration. We analyzed if there was a change in levels or localization of ATXN1. Surprisingly, we found that increased levels of either *Drosophila* KPNA6 (kap-α1) or human KPNA2 resulted in decreased nuclear localization of ATXN1 (82Q) and increased accumulation of ATXN1 in the cytoplasm, in the form of small aggregates (**Figure 4**). Quantification of confocal images confirmed that ATXN1 intensity was lower in the nuclei of neurons co-expressing ATXN1 (82Q) together with KPNAs (**Figure 4, E-F**). These same neurons displayed increased cytoplasmic ATXN1 signal (**Figure 4, G-H**). Given that increased KPNA levels also suppressed neurodegeneration, these results suggest that rather than increasing nuclear translocation, KPNA expression caused mutant ATXN1 (82Q) to decrease in the nucleus, preventing its deleterious effects there.

Increased KPNA levels reduce ATXN1 (82Q) soluble oligomers

Our previous results indicate that increased KPNA levels may chaperone ATXN1 (82Q) and limit its translocation to the nucleus. As in other neurodegenerative diseases, soluble ATXN1 (82Q) oligomers are likely the most pathogenic form of aggregates (Lasagna-Reeves et al., 2015). To test whether KPNA expression would have an effect on mutant ATXN1 oligomerization we developed a Homogeneous Time Resolved Fluorescence (HTRF) assay (**Figure 5**). In this assay HTRF signal will only be produced when two ATXN1 (82Q) monomers form a dimer or oligomer. Since a mild detergent (TritonX) is used and the aqueous supernatant is tested, the assay will only be sensing the presence of soluble oligomers. We found that increased levels of the *Drosophila* homologs of KPNA2 (pen), KPNA4 (Kap-α3) and KPNA6 (Kap-α1) as well as human KPNA2, resulted in a decrease in ATXN1 (82Q) soluble oligomer HTRF signal detected in the *Drosophila* head extracts (**Figure 5A**). This result supports that KPNAs are able to prevent ATXN1(82Q) from adopting potentially pathogenic oligomeric conformations.

Discussion

The role played by NCT in neurodegeneration is an expanding area of research (Moore et al., 2020; Fallini et al., 2020). On one hand, many disease driving proteins cause abnormalities in the distribution or the function of NCT proteins or nuclear structures like the nuclear lamina, which are also observed in patients (Sohn et al., 2023; Eftekharzadeh et al., 2018; Woerner et al., 2016; Frost et al., 2016). On the other hand, nucleo-cytoplasmic mislocalization of disease-driving proteins like TDP-43, Tau or Synuclein is observed in patient brains of AD, ALS, FTD or PD (Arai et al., 2006; Eftekharzadeh et al., 2018; Koss et al., 2022). In line with this, the abnormal nuclear or cytoplasmic localization of the disease driving proteins influences their toxicity (Rousseaux et al., 2016; Guo et al., 2018; Klement et al., 1998).

Increasing KPNB levels has been previously shown to modulate the neurodegeneration caused by the neurodegeneration-inducing protein like TDP-43 and ATXN3 (Khalil et al., 2022; Pasha et al., 2021; Sowa et al., 2018; Aveditashi et al., 2022). Here we show for the first time that increasing the levels of KPNAs ameliorates the neurodegeneration induced by mutant ATXN1. Interestingly, whereas the protective effect of increased KPNB levels is associated with its ability to relocate TDP-43 back to the nucleus (Khalil et al., 2022), this is not the case in the KPNA-ATXN1 interaction. Rather, increased KPNA levels result in the retention of mutant ATXN1 in the cytoplasm and its decrease in the nucleus. Even though the protective effect of mutating the NLS sequence in ATXN1 has been previously demonstrated (Klement et al., 1998; Handler et al., 2023), our observations constitute a proof of principle that genetic or pharmaceutical manipulations that prevent the nuclear translocation of mutant ATXN1 (still having a functioning NLS) should lead to neuroprotection in the context of SCA1, pointing to an attractive therapeutic avenue.

It has been suggested that NIRs can act as chaperones with the ability to disaggregate disease driving proteins (like TDP-43) before transporting them to the nucleus (Khalil et al., 2022; Fare et al., 2023; Girdhar & Guo, 2022; Pasha et al., 2021; Guo et al., 2018). Our observations in the context of the ATXN1-KPNA interaction suggest that the protective chaperoning ability of NIRs can be uncoupled from the nuclear transport function. This is supported by the fact that we see less nuclear ATXN1, not more, and more cytoplasmic ATXN1, when the levels of KPNA are increased. Additionally, we observe a statistically significant decrease in ATXN1 soluble oligomers when the levels of KPNA are increased. Taken together, our results suggest that the binding of mutant ATXN1 and KPNA results in cytoplasmic aggregates that are not toxic and a decrease in toxic oligomers.

Several neurodegeneration driving proteins including mutant ATXN1 have the capacity to interfere with NCT (Zhang, Williamson, et al., 2020; Ding & Sepehrimanesh, 2021; Eftekharzadeh et al., 2018; Woerner et al., 2016). Therefore, it is possible that part of the neuroprotective effects of increasing KPNA in our assays is due to the partial restoration of NCT to more normal levels. This possibility is outside of the scope of this work but will be the subject of future research once we establish a *Drosophila* strain allowing for the assessment of NCT in the context of mutant ATXN1.

Tau and Synuclein are normally cytoplasmic but have been observed in the nuclei of tauopathy and PD neurons respectively (Eftekharzadeh et al., 2018; Candia et al., 2022; Koss et al., 2022). Furthermore, their nuclear translocation, mediated by TRIM28 for example, results in an

exacerbated toxicity (Rousseaux et al., 2016). Additionally, Tau has been shown to interact with NUP98 which promotes its aggregation (Eftekharzadeh et al., 2018) and KPNA and KPNB levels and nucleocytoplasmic distribution are altered in many diseases including AD (Nuovo et al., 2017; Pasha et al., 2021). This suggests that the neuroprotective role of KPNAs in the context of neurodegenerative diseases may extend beyond our observations in the context of SCA1, having broader implications.

Materials and methods

Drosophila strains: Alleles expressing the different KPNA variants used where obtained from the Bloomington Drosophila Stock Center (BDSC). The *UAS-ATXN1 (82Q) F7* strain was used for all experiments (Fernandez-Funez et al., 2000). *GMR-GAL4* (Freeman et al., 1996) was used to drive expression of ATXN1 (82Q) in the retina while *nrv2-GAL4* (BDSC line 6800) was used to drive ATXN1 (82Q) in the nervous system.

Immunofluorescence: Ten-day old *Drosophila* CNS was dissected in cold PBS and fixed in 4% formaldehyde/PBS for 25 mins at room temperature. Tissue was incubated in primary antibody overnight at 4°C. We used 11NQ anti-ATXN1 as previously described (Al-Ramahi et al., 2006) and rat anti-HA (Sigma, clone 3F10). Following washes, Alexa Fluor 488 and Alexa Fluor 555 secondary antibodies (Thermo Fisher Scientific) were used and Dapi was added to stain the nuclei. Images were captured using a Leica SP8 confocal system.
In order to quantify the nucleocytoplasmic distribution of ATXN1, we used ImageJ to create a mask using the Dapi signal. This allowed for the separate quantification of nuclear and cytoplasmic ATXN1 signal. The ImageJ Analyze Particles plugin was used to quantify the individual signal of each nucleus in order to generate the distribution.

External eye images and retinal sections: For external eye images, the fruit flies were raised at 29°C. Images were captured using the Leica MZ16 imaging system. For retinal sections, animals were fixed (85% ethanol, 3.7% Formaldehyde, 5% Acetic Acid) overnight at room temperature. Tissue was dehydrated, embedded in paraffin and sectioned in 10uM slices. Following deparaffinization and rehydration, slides were stained using Harris hematoxylin and mounted using Permount medium.

Drosophila motor performance assay: To assess motor performance of fruit flies as a function of age, we used ten age-matched females per replica per genotype as previously described (Onur et al., 2021). Flies were collected over a 24 hour period and transferred into a new vial containing 300 µl of media every day. Animals were kept at 28°C. Four replicates were used per genotype. Using an automated platform, the animals are taped to the bottom of a plastic vial and recorded for 7.5s as they climb back up on the walls of the vials. Videos are analyzed using custom software to assess the speed of each individual animal. Four trials per replicate are performed each day shown, and four replicates per genotype are used. Using the average performance of all 10 animals in each replicate and 4 replicates per genotype, a nonlinear random mixed effect model ANOVA was applied to the average using each four replicates to establish statistical significance across genotypes. P-values were adjusted for multiplicity using Holm's procedure. Code for this analysis is available upon request. All graphing and statistical

analyses were performed in R. A neutral UAS line was used to generate negative controls to establish the healthy baseline motor performance and disease controls for the disease baseline.

Homogeneous Time Resolved Fluorescence: 11NQ antibody was labeled (Cisbio-Revvity) with Europium Cryptate (donor fluorophore) or with D2 (acceptor fluorophore). 42 heads per genotype were homogenized in 60ul of extraction buffer (1% TritonX in PBS + Protease inhibitor) and incubated at 4°C overnight. Readings were performed in triplicates of 20ul containing a 1:50 dilution of the extracts and 2ul of each labeled antibody. HTRF was evaluated using a Tecan Infinite® 200 PRO following the setting recommended by Cisbio-Revvity. In addition to the ATXN1 oligomerization HTRF signal calculation, controls of the exact same genotype but not expressing ATXN1 were used as blanks to account for background fluorescence.

FIGURE 1. KPNAs interact with ATXN1 (82Q) in the nucleus & the cytoplasm in the *Drosophila* CNS. Confocal images of *Drosophila* neurons in the adult ventral nerve cord (VNC) stained with anti-ATXN1 (82Q) antibody (green), antibodies staining different KPNA proteins (red) and DAPI marking the nuclei (blue). (**A**) No ATXN1 (82Q) (green) or KPNA staining (red) is detected in negative controls. (**B**) ATXN1 (82Q) staining (green) detected in discrete aggregates. (**C - E**) Reveal colocalization of ATXN1 (82Q) with either *Drosophila* Kap-α1 (**C**) or human overexpressed KPNA5 (**D**) and KPNA2 (**E**). Notice the overlap of the ATXN1 (82Q) and KPNA signals in both the nucleus (*hollow arrows*) and the cytoplasm (*solid arrows*) in the merged images. A-E scale bars = 10μm. Flies were raised at 28°C. Transgenes were expressed from the *nrv2-GAL4* driver.

FIGURE 2. Increased levels of KPNAs ameliorate ATXN1 (82Q)-induced photoreceptor degeneration. (**A-H**) External eye images and (**I-P**) retinal paraffin sections from the genotype combinations indicated on the top. Arrows indicate photoreceptor length. (**A and I**) Control eyes show regularly arranged ommatidia, and evenly distributed interommatidial bristles. Control retinas have long, straight, parallel photoreceptors with no gaps between them. (**B and J**) ATXN1 (82Q) eyes have disorganized ommatidia and interommatidial bristles are unevenly distributed or missing (compare B and A). Retinas show fewer photoreceptors that are curved and short (compare J and I). (**C-H** and **K-P**) Amelioration of external and retinal degeneration with increased levels of different *Drosophila* (C-F and K-N) or human (G-H and O-P) KPNAs. Note the improved arrangement of the ommatidia in ATXN1 (82Q) / KPNA animals when compared to ATXN1 (82Q) eyes with endogenous levels of KPNAs (compare C-H with B). Note also the improved retinal organization with longer straight photoreceptors (compare K-P with J). Scale bars on images A-H = 100μm, and on images I-P = 10μm. A-H, done at 29°C. I-P, done at 25°C. Transgenes are expressed from the *GMR-GAL4* eye driver. A neutral UAS line was used for the ATXN1 (82Q)/No modifier control.

FIGURE 3. Increased levels of KPNAs ameliorate ATXN1 (82Q)-induced neuronal dysfunction. (**A-D**) Motor performance quantification in flies of the indicated genotypes measured as speed as a function of age. Control animals perform well in the motor assay for 25 days (blue lines). Flies expressing just ATXN1 (82Q) in the nervous system (gray lines) show progressive motor dysfunction when compared to non-ATXN1 (82Q) controls (blue lines). Co-expression of ATXN1 (82Q) together with KPNAs in the nervous system ameliorates ATXN1 (82Q) induced motor impairments (red lines). Dark lines indicate regression splines and shaded areas are the confidence intervals. Statistical significance between ATXN1 (82Q) alone (gray line) or together with a candidate gene knockdown (red line) is based on a non-linear mixed-effect model ANOVA ($\alpha = 0.05$). Flies were raised at 28°C. The transgenes are expressed using the *nrv2-GAL4* driver line and a neutral UAS line was used for the ATXN1 (82Q)/No modifier control.

FIGURE 4. Increased levels of KPNAs decreases nuclear ATXN1 (82Q) levels. Confocal images of *Drosophila* neurons in the adult VNCs stained with anti-ATXN1 (82Q) antibody (green), and DAPI marking the nucleus (blue). (**A**) No ATXN1 (82Q) (green) is detected in the neurons of negative control animals. (**B**) ATXN1 (82Q) staining (green) detected in discrete aggregates. Notice the ATXN1 (82Q) signal (green) is predominantly localized to the nucleus (blue) in the merged image (**C** and **D**) Notice the decreased nuclear ATXN1 (82Q) signal (arrowheads) and increased cytoplasmic ATXN1 (82Q) signal (small arrows) when ATXN1 (82Q) is expressed alongside different KPNAs (**E** and **F**) Histograms depict the proportion of nuclei as a function of nuclear ATXN1 (82Q) intensity. Notice the shift in the peak proportion of nuclei towards the left (lower ATXN1 levels) in the pink (KPNA expressing) in both graphs, compared to *Drosophila* expressing ATXN1 alone (Grey line). Average nuclear levels of ATXN1 were also significantly decreased (vertical lines). (**G** and **H**) Bar graphs depict the significant increase in cytoplasmic ATXN1 (82Q) when ATXN1 (82Q) is co-expressed with the overexpression of KPNAs. *Lanes* A-D scale bars = 10µm. Flies were raised at 28°C. Transgene expression is achieved using *nrv2-GAL4*, “no modifier” controls express a neutral UAS line. Data in E-H was obtained from quantifying 5 VNCs per genotype. P values correspond to ANOVA followed by Student’s t test. Error bars are standard error of the mean.

FIGURE 5: increased KPNA levels decrease soluble oligomeric mutant ATXN1
(**A**) A Homogeneous Time Resolved Fluorescence (HTRF) experiment was performed to detect soluble ATXN1 (82Q) protein oligomers in fly heads expressing ATXN1 (82Q) either alone (*Lane* 2, no modifier) or in combination with increased KPNA levels (*Lanes* 3-6). Lane 1 displays no ATXN1 (82Q) soluble aggregates in negative controls. ATXN1 oligomers are detected by HTRF in ATXN1 (82Q)-expressing animals. Notice the significant decrease in ATXN1 (82Q) soluble aggregates in lanes 3-6 when ATXN1 (82Q) is co-expressed with karyopherins. Flies were raised at 29°C. **(B)** Illustration showing the design of the oligomeric ATXN1 (82Q) HTRF assay. The same antibody was labeled with Europium Cryptate and with D2, therefore HTRF signal will only take place when two molecules of ATXN1 (82Q) protein are bound to each other. P values represent ANOVA followed by Dunnett’s post-hoc test. Error bars represent the standard error of the mean.

References

Abeditashi, M., Weber, J. J., Pereira Sena, P., Velic, A., Kalimeri, M., Incebacak Eltemur, R. D., Schmidt, J., Hübener-Schmid, J., Hauser, S., Macek, B., Riess, O., & Schmidt, T. (2022). KPNB1 modulates the Machado–Joseph disease protein ataxin-3 through activation of the mitochondrial protease CLPP. *Cellular and Molecular Life Sciences*, *79*(8). https://doi.org/10.1007/s00018-022-04372-5

Al-Ramahi, I., Lu, B., Di Paola, S., Pang, K., de Haro, M., Peluso, I., Gallego-Flores, T., Malik, N. T., Erikson, K., Bleiberg, B. A., Avalos, M., Fan, G., Rivers, L. E., Laitman, A. M., Diaz-García, J. R., Hild, M., Palacino, J., Liu, Z., Medina, D. L., & Botas, J. (2018). High-Throughput Functional Analysis Distinguishes Pathogenic, Nonpathogenic, and Compensatory Transcriptional Changes in Neurodegeneration. *Cell Systems*, *7*(1), 28-40.e4. https://doi.org/10.1016/j.cels.2018.05.010

Arai, T., Hasegawa, M., Akiyama, H., Ikeda, K., Nonaka, T., Mori, H., Mann, D., Tsuchiya, K., Yoshida, M., Hashizume, Y., & Oda, T. (2006). TDP-43 is a component of ubiquitin-positive tau-negative inclusions in frontotemporal lobar degeneration and amyotrophic lateral sclerosis. *Biochemical and Biophysical Research Communications*, *351*(3), 602–611. https://doi.org/10.1016/j.bbrc.2006.10.093

Aramburu, I. V., & Lemke, E. A. (2017). Floppy but not sloppy: Interaction mechanism of FG-nucleoporins and nuclear transport receptors. In *Seminars in Cell and Developmental Biology* (Vol. 68, pp. 34–41). Elsevier Ltd. https://doi.org/10.1016/j.semcdb.2017.06.026

Candia, R. F., Cohen, L. S., Morozova, V., Corbo, C., & Alonso, A. D. (2022). Importin-Mediated Pathological Tau Nuclear Translocation Causes Disruption of the Nuclear Lamina, TDP-43 Mislocalization and Cell Death. *Frontiers in Molecular Neuroscience*, *15*. https://doi.org/10.3389/fnmol.2022.888420

Chan, W. M., Tsoi, H., Wu, C. C., Wong, C. H., Cheng, T. C., Li, H. Y., Lau, K. F., Shaw, P. C., Perrimon, N., & Chan, H. Y. E. (2011). Expanded polyglutamine domain possesses nuclear export activity which modulates subcellular localization and toxicity of polyQ disease protein via exportin-1. *Human Molecular Genetics*, *20*(9), 1738–1750. https://doi.org/10.1093/hmg/ddr049

Coyne, A. N., & Rothstein, J. D. (2022). Nuclear pore complexes — a doorway to neural injury in neurodegeneration. In *Nature Reviews Neurology* (Vol. 18, Issue 6, pp. 348–362). Nature Research. https://doi.org/10.1038/s41582-022-00653-6

Ding, B., & Sepehrimanesh, M. (2021). Nucleocytoplasmic transport: Regulatory mechanisms and the implications in neurodegeneration. *International Journal of Molecular Sciences*, *22*(8). https://doi.org/10.3390/ijms22084165

Eftekharzadeh, B., Daigle, J. G., Kapinos, L. E., Coyne, A., Schiantarelli, J., Carlomagno, Y., Cook, C., Miller, S. J., Dujardin, S., Amaral, A. S., Grima, J. C., Bennett, R. E., Tepper, K., DeTure, M., Vanderburgh, C. R., Corjuc, B. T., DeVos, S. L., Gonzalez, J. A., Chew, J., … Hyman, B. T. (2018). Tau Protein Disrupts Nucleocytoplasmic Transport in Alzheimer's Disease. *Neuron*, *99*(5), 925-940.e7. https://doi.org/10.1016/j.neuron.2018.07.039

Evans, S. M., Rodino, K. G., Adcox, H. E., & Carlyon, J. A. (2018). Orientia tsutsugamushi uses two Ank effectors to modulate NF-κB p65 nuclear transport and inhibit NF-κB transcriptional activation. *PLoS Pathogens*, *14*(5). https://doi.org/10.1371/journal.ppat.1007023

Fallini, C., Khalil, B., Smith, C. L., & Rossoll, W. (2020). Traffic jam at the nuclear pore: All roads lead to nucleocytoplasmic transport defects in ALS/FTD. In *Neurobiology of Disease* (Vol. 140). Academic Press Inc. https://doi.org/10.1016/j.nbd.2020.104835

Fare, C. M., Rhine, K., Lam, A., Myong, S., & Shorter, J. (2023). A minimal construct of nuclear-import receptor Karyopherin-β2 defines the regions critical for chaperone and disaggregation activity. *Journal of Biological Chemistry*, *299*(2). https://doi.org/10.1016/j.jbc.2022.102806

Fernandez-Funez, P., Nino-Rosales, M. L., De Gouyon, B., She, W. C., Luchak, J. M., Martinez, P., Turiegano, E., Benito, J., Capovilla, M., Skinner, P. J., McCall, A., Canal, I., Orr, H. T., Zoghbi, H. Y., & Botas, J. (2000). Identification of genes that modify ataxin-1-induced neurodegeneration. *Nature*, *408*(6808). https://doi.org/10.1038/35040584

Freeman, M. (1996). Reiterative use of the EGF receptor triggers differentiation of all cell types in the Drosophila eye. *Cell*, *87*(4), 651–660. https://doi.org/10.1016/s0092-8674(00)81385-9

Gasset-Rosa, F., Chillon-Marinas, C., Goginashvili, A., Atwal, R. S., Artates, J. W., Tabet, R., Wheeler, V. C., Bang, A. G., Cleveland, D. W., & Lagier-Tourenne, C. (2017). Polyglutamine-Expanded Huntingtin Exacerbates Age-Related Disruption of Nuclear Integrity and Nucleocytoplasmic Transport. *Neuron*, *94*(1), 48-57.e4. https://doi.org/10.1016/j.neuron.2017.03.027

Girdhar, A., & Guo, L. (2022). Regulating Phase Transition in Neurodegenerative Diseases by Nuclear Import Receptors. In *Biology* (Vol. 11, Issue 7). MDPI. https://doi.org/10.3390/biology11071009

Görlich, D., Henklein, P., Laskey, R. A., & Hartmann, E. (1996). A 41 amino acid motif in importin-α confers binding to importin-β and hence transit into the nucleus. *EMBO Journal*, *15*(8), 1810–1817. https://doi.org/10.1002/j.1460-2075.1996.tb00530.x

Guo, L., Kim, H. J., Wang, H., Monaghan, J., Freyermuth, F., Sung, J. C., O'Donovan, K., Fare, C. M., Diaz, Z., Singh, N., Zhang, Z. C., Coughlin, M., Sweeny, E. A., DeSantis, M. E., Jackrel, M. E., Rodell, C. B., Burdick, J. A., King, O. D., Gitler, A. D., … Shorter, J. (2018). Nuclear-Import Receptors Reverse Aberrant Phase Transitions of RNA-Binding Proteins with Prion-like Domains. *Cell*, *173*(3). https://doi.org/10.1016/j.cell.2018.03.002

Handler, H. P., Duvick, L., Mitchell, J. S., Cvetanovic, M., Reighard, M., Soles, A., Mather, K. B., Rainwater, O., Serres, S., Nichols-Meade, T., Coffin, S. L., You, Y., Ruis, B. L., O'Callaghan, B., Henzler, C., Zoghbi, H. Y., & Orr, H. T. (2023). Decreasing mutant ATXN1 nuclear localization improves a spectrum of SCA1-like phenotypes and brain region transcriptomic profiles. *Neuron*, *111*(4), 493-507.e6. https://doi.org/10.1016/j.neuron.2022.11.017

Hergesheimer, R. C., Chami, A. A., De Assis, D. R., Vourc'h, P., Andres, C. R., Corcia, P., Lanznaster, D., & Blasco, H. (2019). The debated toxic role of aggregated TDP-43 in amyotrophic lateral sclerosis: A resolution in sight? In *Brain* (Vol. 142, Issue 5, pp. 1176–1194). Oxford University Press. https://doi.org/10.1093/brain/awz078

Hou, Y., Dan, X., Babbar, M., Wei, Y., Hasselbalch, S. G., Croteau, D. L., & Bohr, V. A. (2019). Ageing as a risk factor for neurodegenerative disease. In *Nature Reviews Neurology* (Vol. 15, Issue 10, pp. 565–581). Nature Publishing Group. https://doi.org/10.1038/s41582-019-0244-7

Huang S, Zhu S, Li XJ, Li S. (2019) The Expanding Clinical Universe of Polyglutamine Disease. *Neuroscientist. 25*(5):512-520. https://doi.org/10.1177/1073858418822993

Ionescu, A., Altman, T., & Perlson, E. (2023). Looking for answers far away from the soma-the (un)known axonal functions of TDP-43, and their contribution to early NMJ disruption in ALS. *Molecular Neurodegeneration*, *18*(1), 35. https://doi.org/10.1186/s13024-023-00623-6

Jäkel, S., Mingot, JM., Schwarzmaier, P., Hartmann, E., & Görlich, D. (2002). Importins fulfil a dual function as nuclear import receptors and cytoplasmic chaperones for exposed basic domains. *The Embo Journal, 21*(3): 377–386. https://doi.org/10.1093/emboj/21.3.377

Khalil, B., Chhangani, D., Wren, M. C., Smith, C. L., Lee, J. H., Li, X., Puttinger, C., Tsai, C. W., Fortin, G., Morderer, D., Gao, J., Liu, F., Lim, C. K., Chen, J., Chou, C. C., Croft, C. L., Gleixner, A. M., Donnelly, C. J., Golde, T. E., … Rossoll, W. (2022). Nuclear import receptors are recruited by FG-nucleoporins to rescue hallmarks of TDP-43 proteinopathy. *Molecular Neurodegeneration*, *17*(1). https://doi.org/10.1186/s13024-022-00585-1

Klement, I. A., Skinner, P. J., Kaytor, M. D., Yi, H., Hersch, S. M., Clark, H. B., Zoghbi, H. Y., & Orr, H. T. (1998). Ataxin-1 nuclear localization and aggregation: Role in polyglutamine- induced disease in SCA1 transgenic mice. *Cell*, *95*(1). https://doi.org/10.1016/S0092-8674(00)81781-X

Koss, D. J., Erskine, D., Porter, A., Palmoski, P., Menon, H., Todd, O. G. J., Leite, M., Attems, J., & Outeiro, T. F. (2022). Nuclear alpha-synuclein is present in the human brain and is modified in dementia with Lewy bodies. *Acta Neuropathologica Communications*, *10*(1), 98. https://doi.org/10.1186/s40478-022-01403-x

Kovacs, G. G. (2016). Molecular pathological classification of neurodegenerative diseases: Turning towards precision medicine. In *International Journal of Molecular Sciences* (Vol. 17, Issue 2). MDPI AG. https://doi.org/10.3390/ijms17020189

Kwong, L. K., Neumann, M., Sampathu, D. M., Lee, V. M. Y., & Trojanowski, J. Q. (2007). TDP-43 proteinopathy: The neuropathology underlying major forms of sporadic and familial frontotemporal lobar degeneration and motor neuron disease. In *Acta Neuropathologica* (Vol. 114, Issue 1, pp. 63–70). https://doi.org/10.1007/s00401-007-0226-5

Lasagna-Reeves, C. A., Rousseaux, M. W. C., Guerrero-Munoz, M. J., Vilanova-Velez, L., Park, J., See, L., Jafar-Nejad, P., Richman, R., Orr, H. T., Kayed, R., & Zoghbi, H. Y. (2015). Ataxin-1 oligomers induce local spread of pathology and decreasing them by passive immunization slows spinocerebellar ataxia type 1 phenotypes. *ELife*, *4*(DECEMBER2015). https://doi.org/10.7554/eLife.10891

Lee, H. gon, Ueda, M., Miyamoto, Y., Yoneda, Y., Perry, G., Smith, M. A., & Zhu, X. (2006). Aberrant localization of importin α1 in hippocampal neurons in Alzheimer disease. *Brain Research*, *1124*(1), 1–4. https://doi.org/10.1016/j.brainres.2006.09.084

March, Z. M., King, O. D., & Shorter, J. (2016). Prion-like domains as epigenetic regulators, scaffolds for subcellular organization, and drivers of neurodegenerative disease HHS Public Access. *Brain Res*, *1647*, 9–18. https://doi.org/10.1016/j.brainres.2016.02.037

Moore, S., Rabichow, B. E., & Sattler, R. (2020). The Hitchhiker's Guide to Nucleocytoplasmic Trafficking in Neurodegeneration. In *Neurochemical Research* (Vol. 45, Issue 6, pp. 1306–1327). Springer. https://doi.org/10.1007/s11064-020-02989-1

Neumann, M., Sampathu, D. M., Kwong, L. K., Truax, A. C., Micsenyi, M. C., Chou, T. T., Bruce, J., Schuck, T., Grossman, M., Clark, C. M., McCluskey, L. F., Miller, B. L., Masliah, E., Mackenzie, I. R., Feldman, H., Feiden, W., Kretzschmar, H. A., Trojanowski, J. Q., & M-Y Lee, V. (2006). *Ubiquitinated TDP-43 in Frontotemporal Lobar Degeneration and Amyotrophic Lateral Sclerosis*. https://www.science.org

Nuovo, G., Amann, V., Williams, J., Vandiver, P., Quinonez, M., Fadda, P., Paniccia, B., Mezache, L., & Mikhail, A. (2018). Increased expression of importin-β, exportin-5 and nuclear transportable proteins in Alzheimer's disease aids anatomic pathologists in its diagnosis. *Annals of Diagnostic Pathology*, *32*, 10–16. https://doi.org/10.1016/j.anndiagpath.2017.08.003

Onur, T. S., Laitman, A., Zhao, H., Keyho, R., Kim, H., Wang, J., Mair, M., Wang, H., Li, L., Perez, A., de Haro, M., Wan, Y.-W., Allen, G., Lu, B., Al-Ramahi, I., Liu, Z., & Botas, J. (2021). Downregulation of glial genes involved in synaptic function mitigates Huntington's disease pathogenesis. *ELife*, *10*. https://doi.org/10.7554/eLife.64564

Park, J., Al-Ramahi, I., Tan, Q., Mollema, N., Diaz-Garcia, J. R., Gallego-Flores, T., Lu, H. C., Lagalwar, S., Duvick, L., Kang, H., Lee, Y., Jafar-Nejad, P., Sayegh, L. S., Richman, R., Liu, X., Gao, Y., Shaw, C. A., Arthur, J. S. C., Orr, H. T., … Zoghbi, H. Y. (2013). RAS-MAPK-MSK1 pathway modulates ataxin 1 protein levels and toxicity in SCA1. *Nature*, *498*(7454). https://doi.org/10.1038/nature12204

Pasha, T., Zatorska, A., Sharipov, D., Rogelj, B., Hortobágyi, T., & Hirth, F. (2021). Karyopherin abnormalities in neurodegenerative proteinopathies. *Brain*, *144*(10), 2915–2932. https://doi.org/10.1093/brain/awab201

Rhine, K., Al-Azzam, N., Yu, T., & Yeo, G. W. (2022). Aging RNA granule dynamics in neurodegeneration. In *Frontiers in Molecular Biosciences* (Vol. 9). Frontiers Media S.A. https://doi.org/10.3389/fmolb.2022.991641

Rousseaux, M. W., De Haro, M., Lasagna-Reeves, C. A., De Maio, A., Park, J., Jafar-Nejad, P., Al-Ramahi, I., Sharma, A., See, L., Lu, N., Vilanova-Velez, L., Klisch, T. J., Westbrook, T. F., Troncoso, J. C., Botas, J., & Zoghbi, H. Y. (2016). *TRIM28 regulates the nuclear accumulation and toxicity of both alpha-synuclein and tau*. https://doi.org/10.7554/eLife.19809.001

Sohn, C., Ma, J., Ray, W. J., & Frost, B. (2023). Pathogenic tau decreases nuclear tension in cultured neurons. *Frontiers in Aging*, *4*. https://doi.org/10.3389/fragi.2023.1058968

Solomon, D. A., Stepto, A., Au, W. H., Adachi, Y., Diaper, D. C., Hall, R., Rekhi, A., Boudi, A., Tziortzouda, P., Lee, Y. B., Smith, B., Bridi, J. C., Spinelli, G., Dearlove, J., Humphrey, D. M., Gallo, J. M., Troakes, C., Fanto, M., Soller, M., … Hirth, F. (2018). A feedback loop between dipeptide-repeat protein, TDP-43 and karyopherin-α mediates C9orf72-related neurodegeneration. *Brain*, *141*(10), 2908–2924. https://doi.org/10.1093/brain/awy241

Tsoi, P. S., Quan, M. D., Ferreon, J. C., & Ferreon, A. C. M. (2023). Aggregation of Disordered Proteins Associated with Neurodegeneration. In *International Journal of Molecular Sciences* (Vol. 24, Issue 4). MDPI. https://doi.org/10.3390/ijms24043380

Winton, M. J., Van Deerlin, V. M., Kwong, L. K., Yuan, W., Wood, E. M. C., Yu, C. E., Schellenberg, G. D., Rademakers, R., Caselli, R., Karydas, A., Trojanowski, J. Q., Miller, B. L., & Lee, V. M. Y. (2008). A90V TDP-43 variant results in the aberrant localization of TDP-43 in vitro. *FEBS Letters*, *582*(15), 2252–2256. https://doi.org/10.1016/j.febslet.2008.05.024

Woerner, A. C., Frottin, F., Hornburg, D., Feng, L. R., Meissner, F., Patra, M., Tatzelt, J., Mann, M., Winklhofer, K. F., Hartl, F. U., & Hipp, M. S. (n.d.). *Cytoplasmic protein aggregates interfere with nucleocytoplasmic transport of protein and RNA*. https://www.science.org

Zhang, S., Hinde, E., Parkyn Schneider, M., Jans, D. A., & Bogoyevitch, M. A. (2020). Nuclear bodies formed by polyQ-ataxin-1 protein are liquid RNA/protein droplets with tunable dynamics. *Scientific Reports*, *10*(1). https://doi.org/10.1038/s41598-020-57994-9

Zhang, S., Williamson, N. A., Duvick, L., Lee, A., Orr, H. T., Korlin-Downs, A., Yang, P., Mok, Y. F., Jans, D. A., & Bogoyevitch, M. A. (2020). The ataxin-1 interactome reveals direct connection with multiple disrupted nuclear transport pathways. *Nature Communications*, *11*(1). https://doi.org/10.1038/s41467-020-17145-0

Zoghbi, H. Y., & Orr, H. T. (1995). Spinocerebellar ataxia type 1. *Seminars in Cell Biology*, *6*(1), 29–35. https://doi.org/10.1016/1043-4682(95)90012-8

Zoghbi, H. Y., & Orr, H. T. (2000). GLUTAMINE REPEATS AND NEURODEGENERATION. *Annu. Rev. Neurosci*, *23*, 217–247. www.annualreviews.org

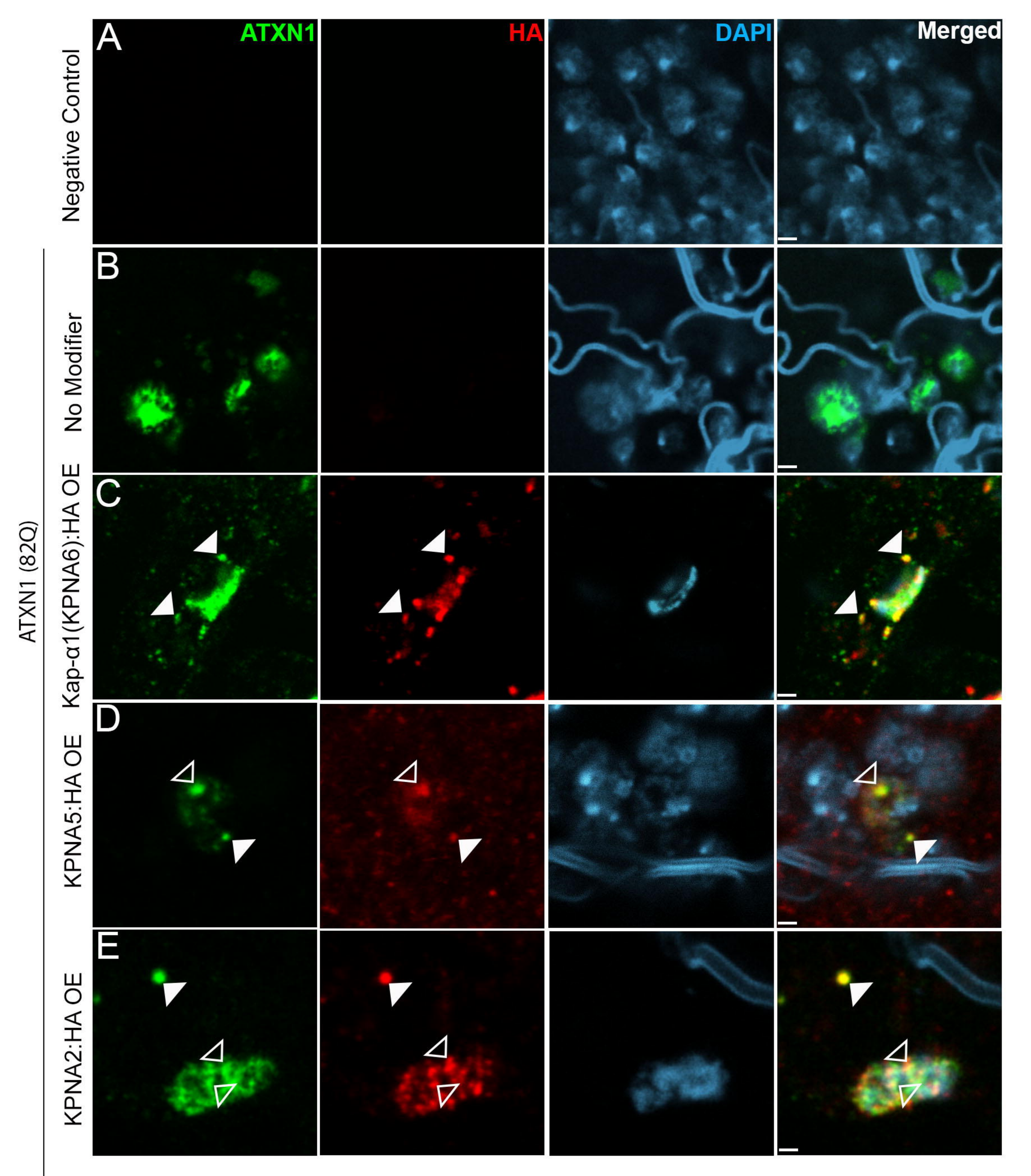
ATXN1
HA
DAPI
Merged
A
Negative Control
B
No Modifier
C
Kap-α1(KPNA6):HA OE
D
KPNA5:HA OE
E
KPNA2:HA OE
ATXN1 (82Q)

ATXN1 (82Q)

Negative Control | No Modifier | Kap-α3(KPNA4) OE | Pen(KPNA2) OE

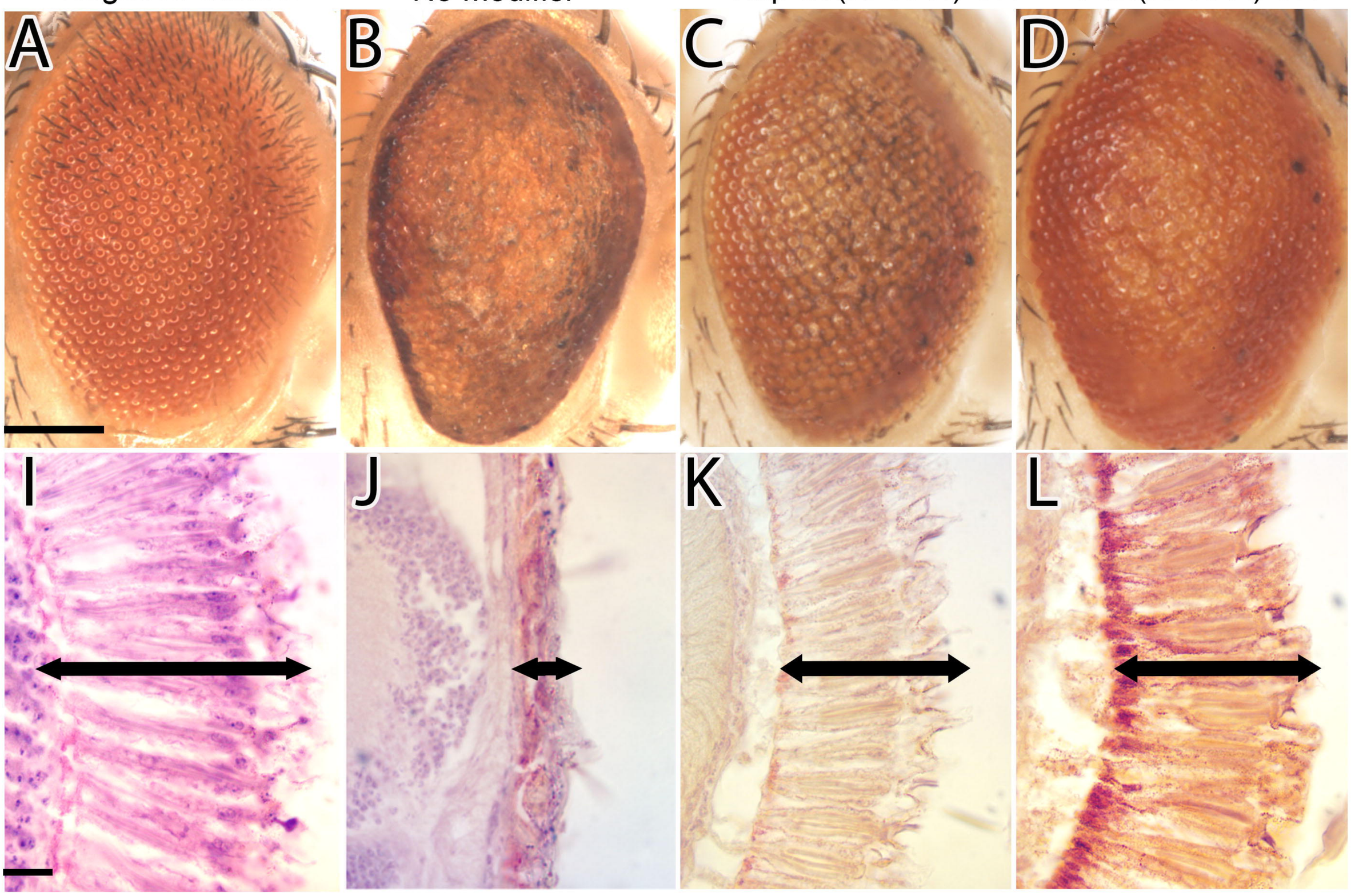

ATXN1 (82Q)

Kap-α1(KPNA6) OE | Kap-α1(KPNA6) OE2 | KPNA5 OE | KPNA2 OE

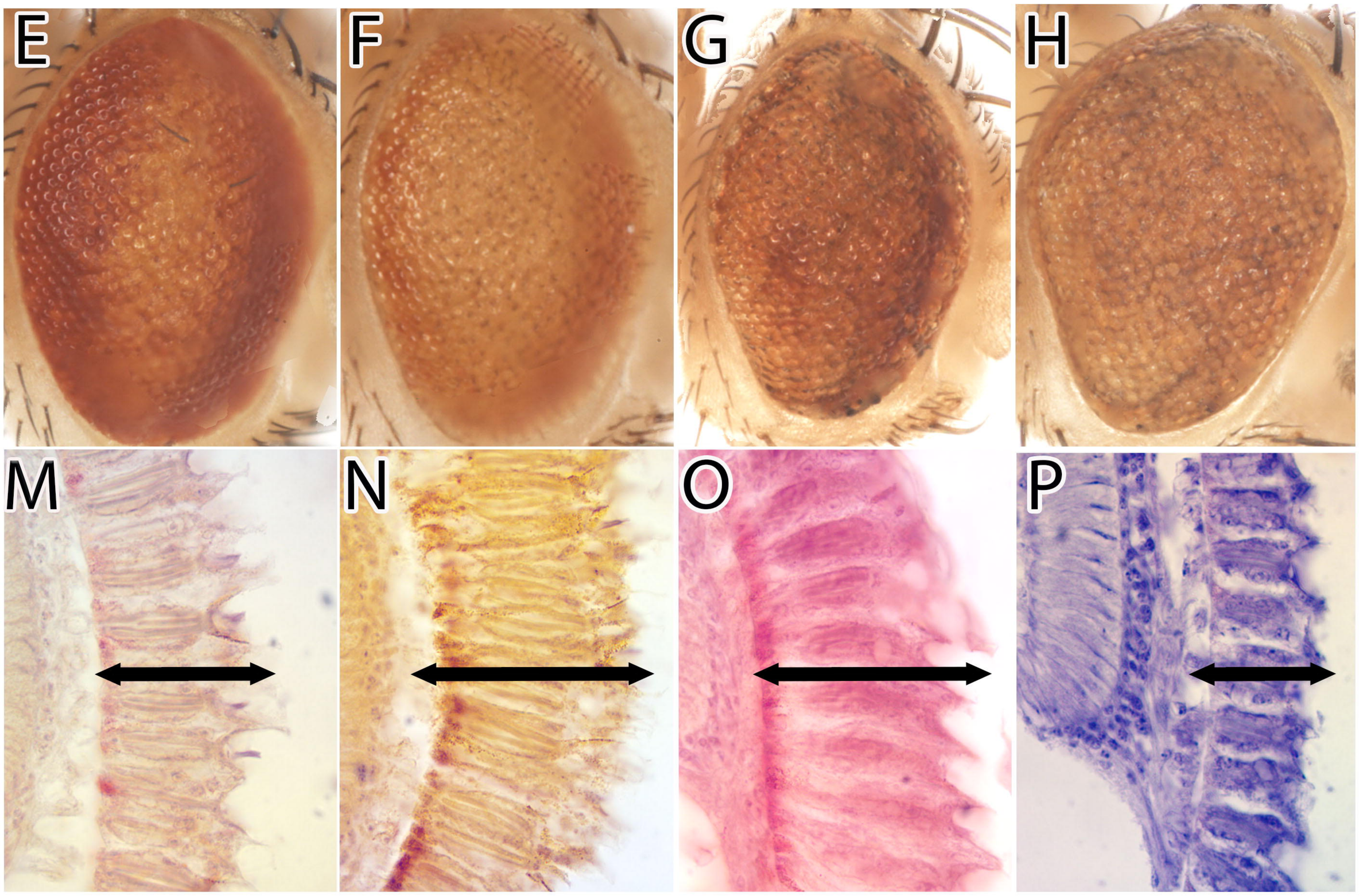

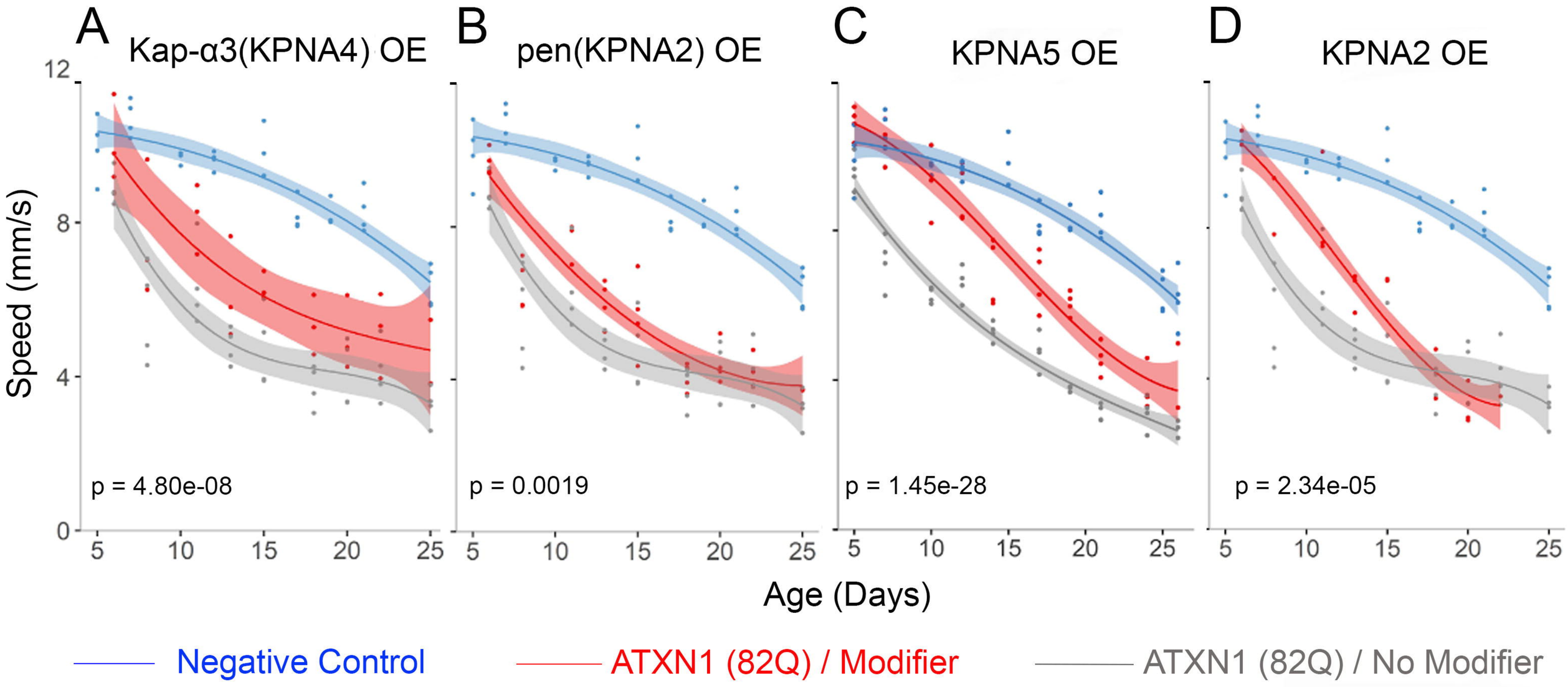
A
Kap-α3(KPNA4) OE
B
pen(KPNA2) OE
C
KPNA5 OE
D
KPNA2 OE
Speed (mm/s)
12
8
4
0
p = 4.80e-08
p = 0.0019
p = 1.45e-28
p = 2.34e-05
5
10
15
20
25
Age (Days)
Negative Control
ATXN1 (82Q) / Modifier
ATXN1 (82Q) / No Modifier

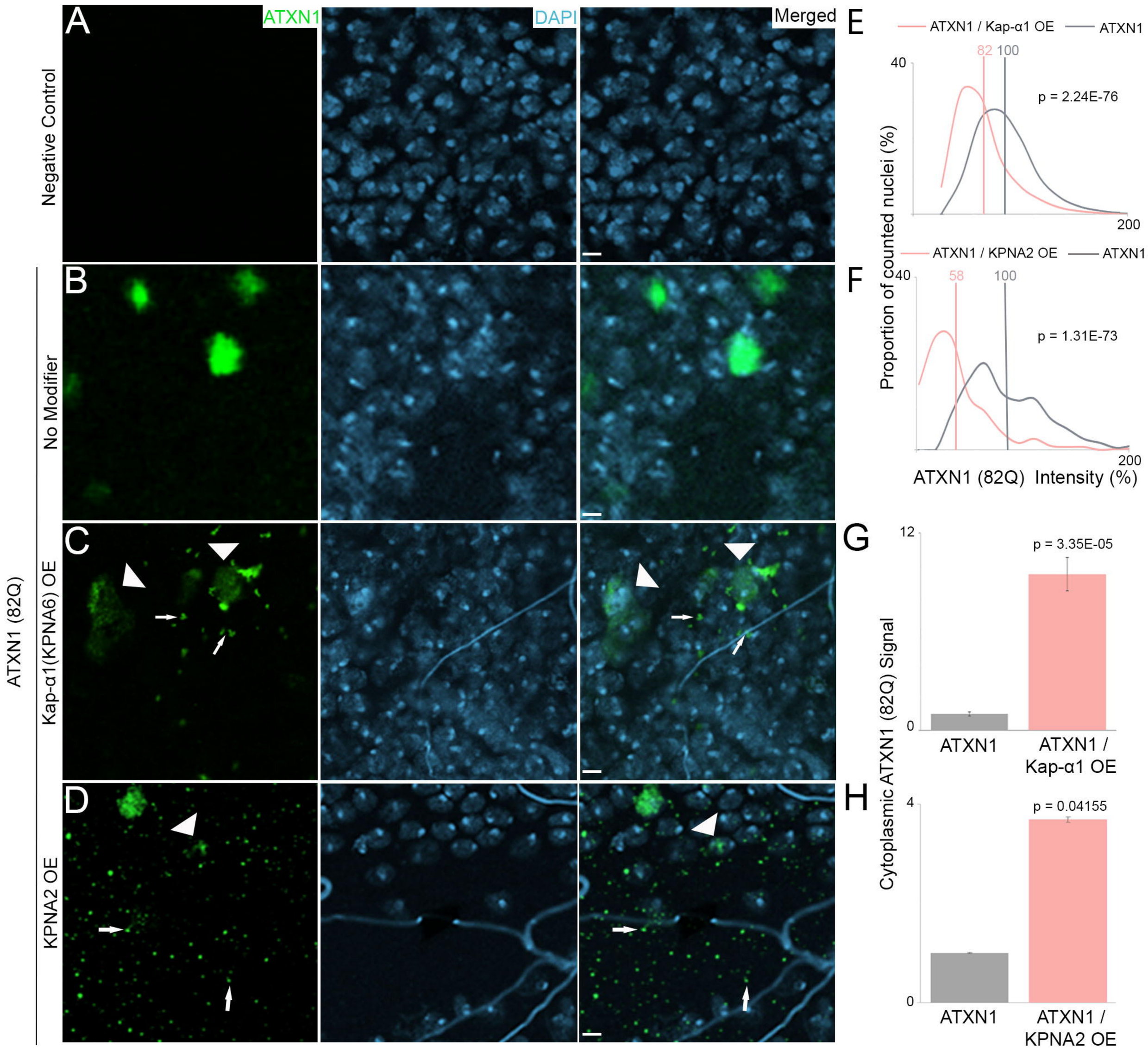
A
ATXN1
DAPI
Merged
Negative Control
B
No Modifier
C
Kap-α1(KPNA6) OE
D
KPNA2 OE
ATXN1 (82Q)
E
ATXN1 / Kap-α1 OE
ATXN1
82
100
40
p = 2.24E-76
200
F
ATXN1 / KPNA2 OE
ATXN1
58
100
40
p = 1.31E-73
200
Proportion of counted nuclei (%)
ATXN1 (82Q) Intensity (%)
G
12
p = 3.35E-05
0
ATXN1
ATXN1 / Kap-α1 OE
Cytoplasmic ATXN1 (82Q) Signal
H
4
p = 0.04155
0
ATXN1
ATXN1 / KPNA2 OE

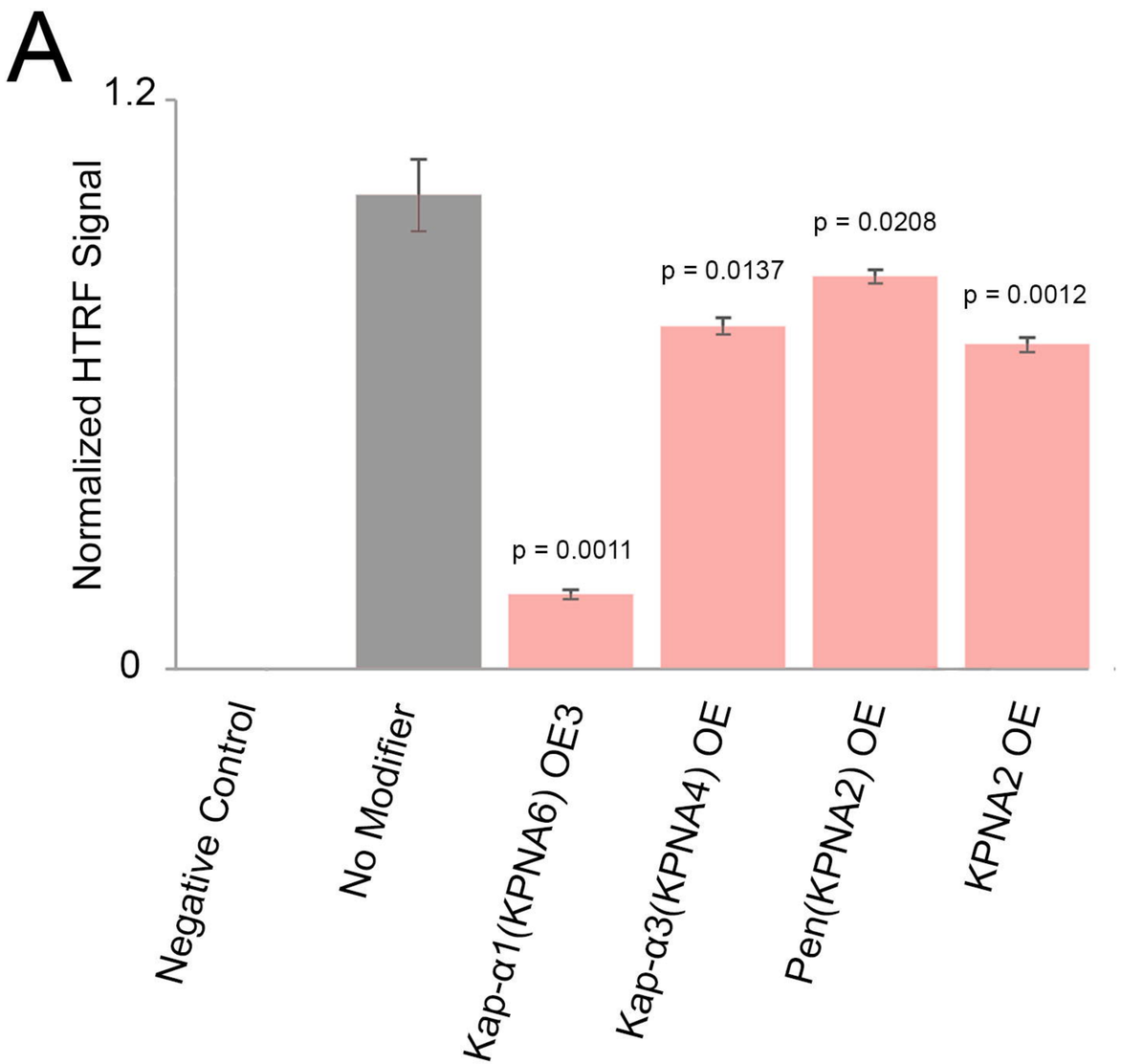
A
1.2
0
Normalized HTRF Signal
p = 0.0011
p = 0.0137
p = 0.0208
p = 0.0012
Negative Control
No Modifier
Kap-α1(KPNA6) OE3
Kap-α3(KPNA4) OE
Pen(KPNA2) OE
KPNA2 OE

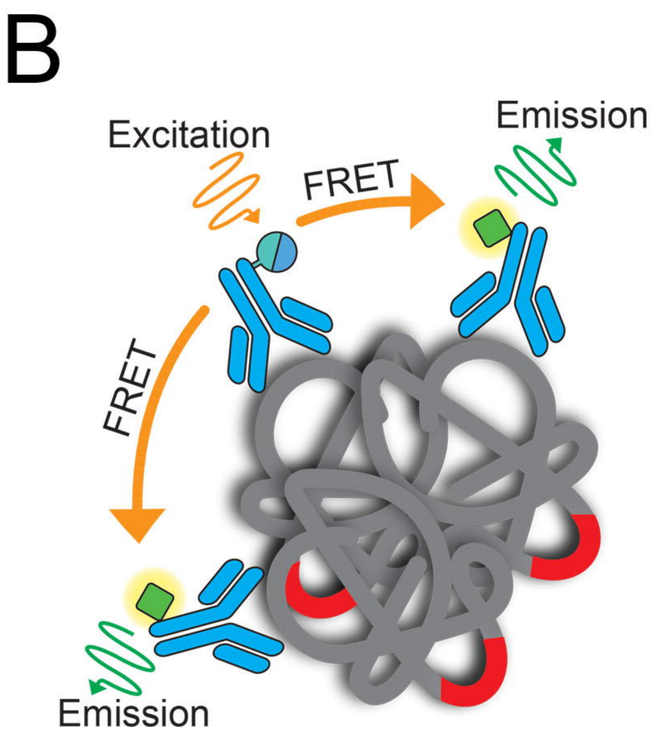
B
Excitation
Emission
FRET
FRET
Emission